Isı Bilimi ve Tekniği Dergisi, 33, 1, 43-53, 2013
J. of Thermal Science and Technology

ISSN 1300-3615

FSI STUDY OF THE EFFECT OF AIR INLET/OUTLET ARRANGEMENTS ON THE RELIABILITY AND COOLING PERFORMANCES OF FLEXIBLE PRINTED CIRCUIT BOARD ELECTRONICS

W.C. LEONG*, M.Z. ABDULLAH, C.Y. KHOR and H.J. TONY TAN
Universiti Sains Malaysia,School of Mechanical Engineering, Engineering Campus, 14300 Nibong Tebal, Penang, Malaysia, *weichiat2008@hotmail.com, Phone: +60 124913898

(Geliş Tarihi: 23.06.2011 Kabul Tarihi: 18.08.2011)

Abstract

Abstract: Flexible printed circuit boards (FPCB) are being used extensively in current electronics devices because of its reduced thickness and ability to bend. Physical reliability and cooling capability are the main concern in the development of FPCB electronics. Therefore, present study investigates the reliability and cooling performance of FPCB, for different air inlet/outlet arrangements, in fan sucking mode. These inlet/outlet arrangements are found to have prominent effect on the performance of FPCB. The FSI (fluid-structure interaction) study is performed using the fluid flow solver FLUENT and structural solver ABAQUS at real-time online coupled by Mesh-based Parallel Code Coupling Interface (MpCCI). In addition, the present study also explores the effect of mass flow rates on the performance of FPCB. As the flow rate increases, the cooling capability is enhanced, but deterioration is observed on the reliability.
Keywords: FSI; flexible printed circuit board; inlet/outlet arrangement; physical reliability; cooling capability.

HAVA GİRİŞ/ÇIKIŞ KONUMLARININ ESNEK DEVRE KARTLARININ GÜVENİLİRLİĞİ VE SOĞUTMA PERFORMANSINA ETKİSİNİN İNCELENMESİ İÇİN AKE ÇALIŞMASI

Özet: Esnek baskılı devre kartları (EBDK), azaltılmış kalınlığı ve esnekliği nedeni ile günümüz elektronik cihazlarında yoğun olarak kullanılmaktadır. Fiziksel güvenilirlik ve soğutulabilme özelliği EBDK elektronik katların geliştirilmesini etkileyen temel unsurlardır. Bundan dolayı, bu çalışmada fan emme durumunda değişik hava giriş/çıkış konumlarının EBDK'nın güvenilirliğine ve soğutulmasına etkisi incelenmiştir. Giriş/çıkış düzenlemelerinin EBDK performansı üzerinde önemli etkileri olduğu bulunmuştur. AKE (akışkan-katı etkileşimi) çalışması, gerçek zamanlı çevrimiçi Mesh-based Parallel Code Coupling Interface (MpCCI) ile akışkan akışı çözücüsü FLUENT ve yapısal çözücü ABACUS birlikte kullanılarak yapılmıştır. Ek olarak, kütlesel debinin EBDK'nın performansına etkileride incelenmiştir. Debi artarken, soğutma kapasitesinin artığı fakat güvenilirliğin azaldığı gözlemlenmiştir.
Anahtar Kelimeler: AKE, Esnek baskılı devre kartı, giriş/çıkış düzenlemesi, fiziksel güvenilirlik, soğutma kapasitesi.

INTRODUCTION

Flexible printed circuit boards (FPCB) can be an alternative to rigid printed circuit board (PCB). It has been proven advantageous in some applications because of its excellent flexibility, twistability and light weight. In the majority of systems with moderate heat dissipation, fans are the most common devices used for cooling purpose. The fan flows can induce pressure on the electronic components and subsequently cause deflection on the board. Compared with rigid board, FPCB experiences much larger deformation during operation and also exhibits different cooling capability. Therefore, durability and long-term performance are the primary concern in the application of FPCB. Many researchers have focused on this area; a review of previous works, which build a background for the current study, is presented as follows.

Azar and Russell (1990) experimentally studied the impact of component layout and geometry on flow distribution on a circuit pack. They found that the flow in electronic enclosures was highly three dimensional, and the location and orientation of components with large aspect ratio would significantly affect the flow distribution. Similar study was reported by Lee and Mahalingam (1993), who used a computational fluid dynamics (CFD) tool to evaluate the velocity and the temperature fields of air flow in a computer system enclosure, and correlated the predictions with real time experiments.

Dealing with the component-PCB heat transfer, Rodgers and co-workers (Eveloy *et al.*, 2000; Rodgers *et al.*, 2003a; Rodgers *et al.*, 2003b) performed numerical and experimental works to assess the predictive accuracy of CFD tools for the thermal analysis of electronic systems, in natural and forced convection modes. The

numerical analysis was performed using the widely used CFD code, i.e. FLOTHERM Versions 1.4 and 2.1. They studied the characterization of the airflow patterns around PCB-mounted electronic components using three complimentary flow visualization techniques, such as smoke-flow and paint-flow visualization techniques, and the paint-film evaporation technique (Lohan *et al.*, 2002). A numerical solution of steady-state forced convection for air flows through a horizontally oriented PCB assembly under the laminar flow conditions was developed by Leung *et al.* (2000). Shankaran and Karimanal (2002) proposed the "zoom-in modeling", a multi level approach with the exact boundary conditions used, for accurate and time efficient CFD design calculations for a populated system cooled by forced air flow. Finite volume method (FVM) based CFD software ICEPAK was used for modeling and simulation. Modeling of forced convection cooling was also reported by Baelmans *et al.* (2003), who observed that fan induced swirling flows were difficult to predict with standard k-ε turbulence models. In addition, Cole *et al.* (2003) investigated the aerodynamic and thermal interactions of ball grid array packages in a real environment. The effect of airflow and PCB thermal conductivity on the junction temperature were analyzed.

Extensive experiments and modeling of flow and heat transfer in axial flow fan cooled electronic systems have been reported by Grimes and co-workers (Grimes *et al.*, 2001; Grimes and Davies, 2002; Grimes *et al.*, 2004a, 2004b). Experiments were conducted in fan sucking (fan mounted at the system outlet) as well as the fan blowing (fan mounted at the system inlet) modes. It was observed that the flow in sucking mode was steady, uniform and easily predictable using a laminar model, whereas in blowing, it was unsteady, swirling and too complex to be predicted by a turbulent model with reasonable accuracy. However, the heat transfer was enhanced by shifting the fan from exit (sucking) to the inlet (blowing).

Few researchers have focused on the material and structural characteristics of FPCB. Li and Jiao (2000) had studied the effects of temperature and aging on the Young's moduli of polymeric based flexible substrates, such as polyethylene naphthalate, polyester and polyimide, using the Dynamic Mechanics Analyzer (DMA). Huang *et al.* (2009) had simulated the mechanical reliability of a BGA mounted on FPCB under drop impact, and found that the stress could be reduced by increasing the height of solder joints. Han *et al.* (20047) also experimentally studied the fatigue behavior of thin Cu foil for FPCB. Interestingly, Barlow *et al.* (2002) demonstrated the feasibility and viability of FPCB for miniaturized electronic assemblies. Siegel *et al.* (2010) were able to fabricate several low-cost flexible electronic circuits on the paper substrates.

For PCB, Leicht and Skipor (2000) experimentally studied the bending fatigue issues of BGA (ball grid array), micro-BGA, CSP (chip scale package), and DCA (direct chip attach) packages mounted on PCB. The fatigue fracture morphology and its relation to solder joint location and rate of crack growth were analyzed. Using FEM model, Shetty *et al.* (2001) focused on the effect of quasi-static bending loads on the durability of 0.5 mm pitch CSP interconnects when assembled on FR4 substrates. Shetty and Reinikainen (2003) conducted three-point and four-point bending tests to evaluate the reliability of CSPs. They formulated a reliability model using FEM and verified with experimental results. Furthermore, Lau *et al.* (2006) had studied PBGA package assemblies under 3-point bending condition, by experiment and simulation.

Recently, Arruda *et al.* (Arruda *et al.*, 2009a; Arruda et al., 2009b) studied flex-rigid PCB (RFPCB) interface to evaluate the cracking phenomena during thermal cycling, using FEM. They found that high stresses could cause micro cracks in the connection between rigid and flex boards. The development of stress was attributed to the design of the PCB and the non-uniformity in thermal expansion of various parts. Sun *et al.* (2009) found by FE analysis that there were some risk places for potential failures, such as the comers of the connecting part of the RFPCB. Accordingly, they obtained the optimized structure through simulations, by simultaneously considering bending, tension and twisting load conditions. Yu *et al.* (2010) analyzed the full-field dynamic responses of PCBs of product level by using digital image correlation technique. Das et al. (2010) obtained that the flexibility of FPCB was decreased with increasing number of metal layers. They were also able to fabricate the biocompatible FPCB on the polydimethylsiloxane (PDMS) substrate.

However, as far as the authors are aware, no previous work has been reported on the effect of air inlet/outlet arrangements on the FPCB electronics. Therefore, the present study is aimed to evaluate the physical reliability and cooling capability of FPCB, for different inlet/outlet arrangements, in fan sucking mode. The understanding of this issue is important because the designer usually has flexibility in determining the sites for the air to enter and vent, in an electronic system. This fluid-structure interaction (FSI) study can also provide better perception on the responses of FPCB electronics under fan-cooled systems. In addition, the effect of air flow rates for one case (axial flow) is also investigated. These studies are carried out using FLUENT and ABAQUS; they are real-time online coupled by Mesh-based Parallel Code Coupling Interface (MpCCI). The flow is assumed to be three dimensional, laminar, incompressible and unsteady.

SIMULATION TOOLS

The FSI study is carried out by using fluid solver FLUENT 6.3.26 and structural solver ABAQUS/CAE 6.9; they are real-time online coupled by MpCCI 3.1.0. Using the MpCCI, the quantities are exchanged from one solver to the other solver via association (neighborhood search) and interpolation. In the present study, the air

flow is solved by FLUENT and then the deformation of FPCB is addressed by ABAQUS as shown in Figure 1.

In the FLUENT solver, the governing equations describing the fluid flow are conservation of mass (continuity equation), conservation of momentum (momentum equation) (Fluent, 2012a) and conservation of energy (energy equation) (Fluent 2012b).

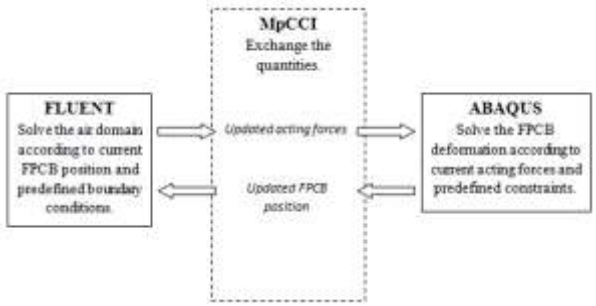

Figure 1. FSI simulation.

The continuity equation is:

$$\frac{\partial \rho_f}{\partial t} + \nabla.\left(\rho_f \overrightarrow{u_f}\right) = 0 \quad (1)$$

where ρ_f is the density of fluid, $\overrightarrow{u_f}$ is the overall velocity vector of fluid and t is the time. Equation (1) is the general form of mass conservation equation and valid for incompressible and compressible flow.

The momentum equation in an inertial (non-accelerating) reference frame is:

$$\rho_f \left(\frac{\partial \overrightarrow{u_f}}{\partial t} + \overrightarrow{u_f}.\nabla \overrightarrow{u_f}\right) = -\nabla P + \nabla.\bar{\bar{\tau}} + \rho_f \vec{g} + \vec{F} \quad (2)$$

where the P is the static pressure, $\bar{\bar{\tau}}$ is the stress tensor, $\vec{g}$ is the gravitational acceleration and $\vec{F}$ is the external body forces.

The energy equation is:

$$\rho_f c_{pf} \left(\frac{\partial T_f}{\partial t} + \overrightarrow{u_f}.\nabla T_f\right) = k_f \nabla^2 T_f \quad (3)$$

where c_{pf} is the specific heat of fluid, k_f is the thermal conductivity of fluid and T_f is the temperature of fluid.

In the ABAQUS solver, the governing equation describing the structure is conservation of momentum (Bielecki et al., 2001).

The momentum equation is:

$$\rho_s \left(\frac{\partial \overrightarrow{u_s}}{\partial t} + \overrightarrow{u_s}.\nabla \overrightarrow{u_s}\right) = -\nabla \vec{\sigma} + \rho_s \vec{g} \quad (4)$$

where ρ_s is the density of solid, $\overrightarrow{u_s}$ is the overall velocity vector of solid, and $\vec{\sigma}$ is the recoverable stresses.

NUMERICAL ANALYSIS

Computational Models

As illustrated in Figure 2, the geometry of the test FPCB in the present study is similar as employed by Grimes and Davies (2004a, 2004b), except that the rigid PCB is replaced by FPCB. The FPCB is accommodated with 15 components with size of 31 mm × 31 mm × 2 mm for each component. Those components are named according to their row and column number; for example first row and second column component is denoted as C1,2. The FPCB is constrained at four corners and they are named as Fix 1, Fix 2, Fix 3 and Fix 4. The Reference line shown is located 12 mm above the circuit board and it is aligned at the centre of row 2 components.

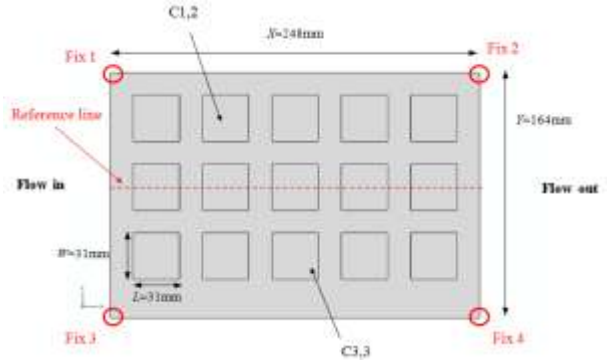

Figure 2. Test FPCB.

In FLUENT, the air domain is meshed with 143,964 hexagonal grids, as depicted in Figure 3. The three dimensional computational model is considered as incompressible, unsteady and laminar flow. For the highest mass flow rate in the present study, the Reynolds number used based on component height is 687 (Lohan *et al.*, 2002). The fan sucking system has been applied similar to Grimes *et al.* (2001) and Grimes and Davies (2000; 2004a; 2004b). The heat transfer coefficient, h is calculated using Equation 5:

$$h = \frac{q}{A\Delta T} \quad (5)$$

where q is the heat flow, A is the area and ΔT is the temperature difference. The enclosure is redesigned with five different air inlet/outlet arrangements as shown in Figure 4, namely Case A (axial flow), Case B (Z-flow perpendicular to FPCB), Case C (U-flow perpendicular to FPCB), Case D (Z-flow parallel to FPCB) and Case E (U-flow parallel to FPCB). The dimensions of the inlets and outlets are fixed at 200 mm × 200 mm. Moreover, effect of flow rates is also investigated on Case A at 0.05 kg/s, 0.10 kg/s, 0.15 kg/s, 0.20 kg/s and 0.25 kg/s. These flow rates are within the typical velocity found in the electronic systems (Cole *et al.*, 2003). The heat flux generated by each component is 461 W/m^2, and the air flow is drawn from ambient with temperature of 21 ^{o}C. The boundary conditions are applied as the following:

a) On component wall: $\vec{u}$=0, $\vec{q}$=461

b) On other wall: $\vec{u}$=0, $\frac{\partial T}{\partial \eta} = 0$

c) At inlet: mass flow rate=$\dot{m}$, T=T_{in}

d) At outlet: P=0

In ABAQUS, the FPCB with components is meshed with 3,027 hexagonal elements, as shown in Figure 5. The fully constraint boundary condition (U_x=U_y=U_z=UR_x=UR_y=UR_z=0) is assigned to the four corners of the FPCB, in which U is the linear displacement and UR is the rotational displacement. The gravity is defined in the negative y-direction. In the

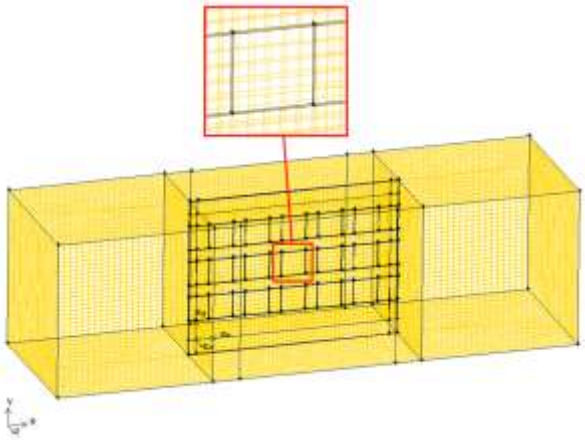

Figure 3. 3-D meshed model in FLUENT.

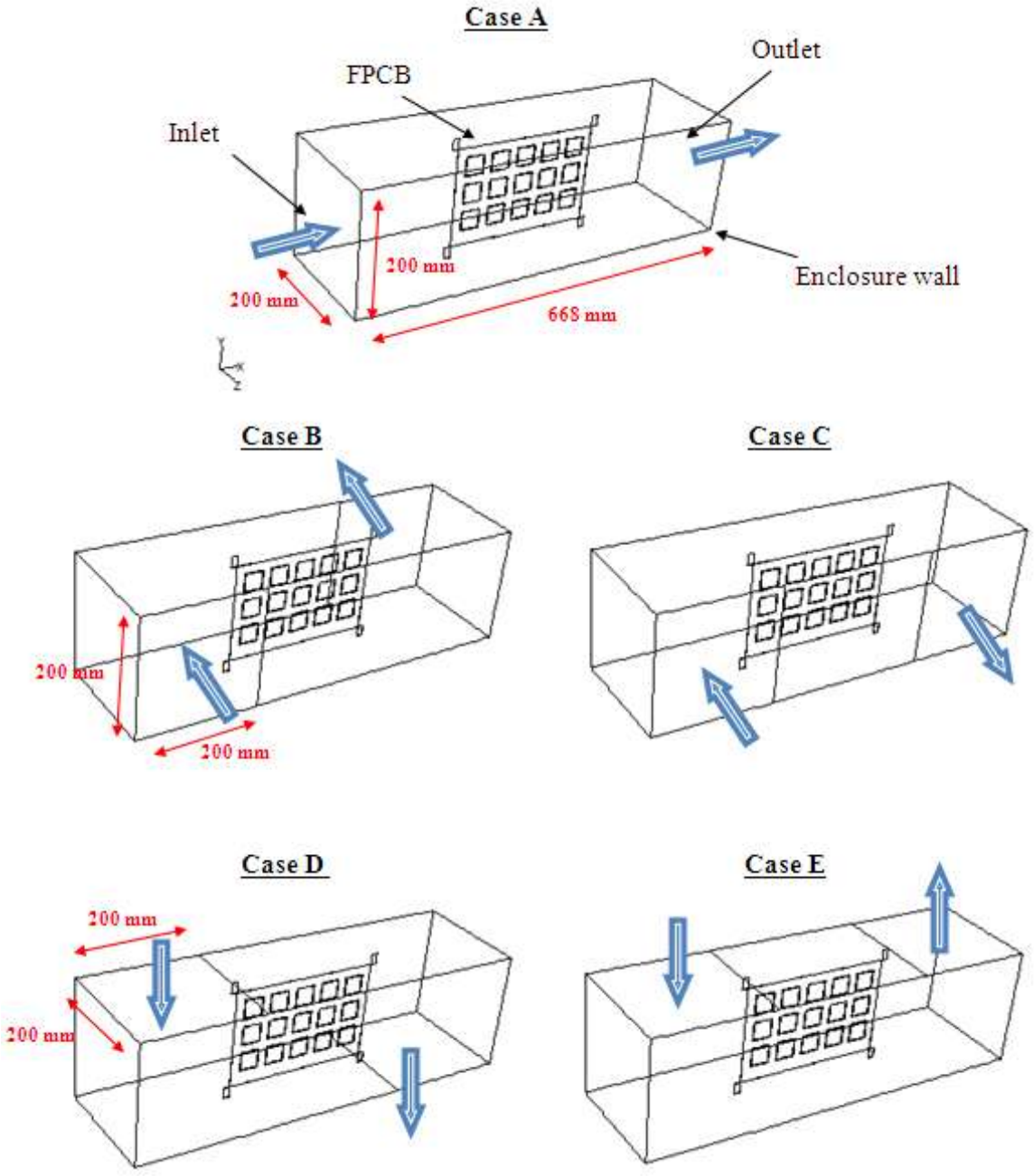

Figure 4. Different air inlet/outlet arrangements.

present study, the FPCB is considered as single layer of polyimide with thickness of 0.2 mm. Since epoxy molding compound (EMC) is the dominating volume, the components are treated as purely EMC. Consideration of multilayer on the component and FPCB is avoided to save computational time and also to reduce the model complexity. The elastic modulus (E), Poisson ratio (υ), and density (ρ) of the materials are defined as in Table 1.

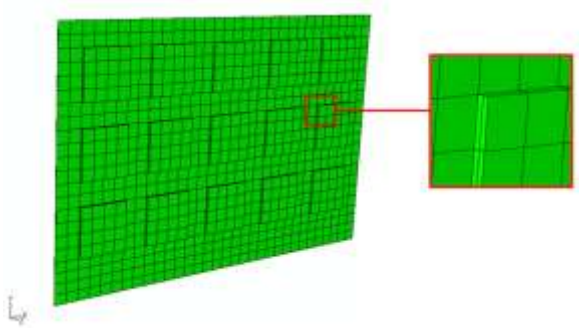

Figure 5. 3-D meshed model in ABAQUS.

Table 1. Material properties (Arruda *et al.*, 2009; Yeh *et al.*, 2006; Odegard *et al.*, 2005).

Parts	Model	E (GPa)	υ	ρ (kg/m^3)
Polyimide FPCB	Isotropic	2.3	0.34	1330
Components	Isotropic	28	0.35	1890

Time Step Independence Test

Firstly, a few time steps are tested out, at a particular number of meshes, to obtain the optimum time step for these computational models. In general, the smaller time step is believed to have a better accuracy. This test is performed on Case A at 0.20 kg/s, and the resulted deflections at C2,3 are shown in Figure 6. In this paper, the deflection is defined as the displacement in the z-direction. It is clearly seen that, the solutions of time step 1 s and 0.1 s behave differently to the solution of time step 0.001 s. However, the solution of time step 0.01 s predicts well the constant-state value. It also demonstrates almost similar trend at the transient state even though it decays faster. With the computer machine with Dual-Core CPU 3.33 GHz and 3 GB RAM, time step 0.001 s requires 96 hours to complete the computation, whereas time step 0.01 s takes only 10 hours to complete. Thus, time step 0.01 s is employed thoroughly in the present study in order to optimize between the accuracy and computational time.

Grid Independence Test

Grid independence test is performed to obtain the optimum mesh size for the models. This test is performed independently on each fluid domain and solid domain for Case A at 0.20 kg/s. In the test, the meshes have been improved throughout the entire domain, including the near wall region. When the mesh number is increased, the meshes at every local part near to the wall are also refined. This makes the calculations

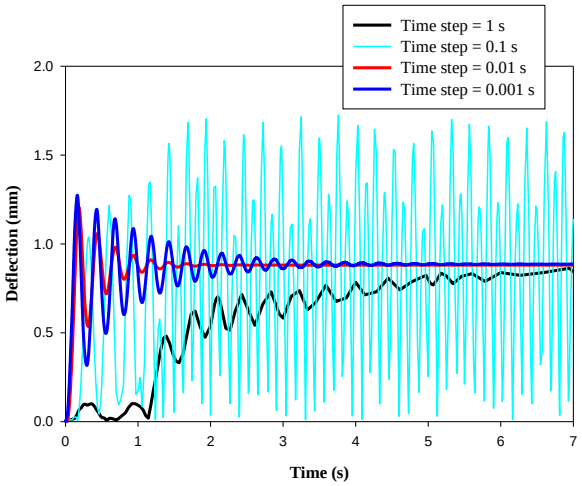

Figure 6. Deflections at different time steps for Case A at 0.20 kg/s.

in the boundary layer region better predicted and hence improves the overall computational accuracy. Similar method is also used by the previous works (Lee and Mahalingam, 1993; Rodgers *et al.*, 2003a; Grimes *et al.*, 2001). The fluid domain mesh is tested for 107974, 128914, 143964 and 165034 grids, with constant solid mesh of 1888. On the other hand, the solid domain mesh is tested for 472, 1888, 3072 and 4152 grids, with constant fluid mesh of 128914. The constant-state value is the value where the deflection reached is constant with time as shown in Table 2. The results are shown that the fluid domain with 143,964 grids and solid domain with 3,072 grids are reasonable to be employed in the present study.

Table 2. Constant-state deflection for different number of grids for Case A at 0.20 kg/s.

Fluid domain grids	Constant-state deflection (mm)	Solid domain grids	Constant-state deflection (mm)
107,974	0.854	472	0.623
128,914	0.860	1,888	0.860
143,964	0.873	3,072	0.887
165,034	0.874	4,152	0.887

Model Validation

The present FSI numerical model is validated against previous experimental work by Grimes and Davies (2004a; 2004b). They conducted the test on PCB at the flow rate of 0.04594 kg/s, as depicted in Figure 7. The flow is compared along the Reference line as indicated in Figure 2. Figures 8 and 9 illustrate the comparisons of flow velocity and component temperature between the present FSI simulation and the experimental data. It is found that, the present simulation and the experimental results show good agreement in terms of trend and magnitude for both temperature and axial velocity. The average discrepancy magnitude is below 10% for air flow and below 4% for temperature. These discrepancies may due to several simplifications made in the current FSI simulation, such as neglecting of swirl and radial flow for the exhaust fan, assumption that the

heat is dissipated uniformly from the component surface, and neglecting of air gaps between components and the board.

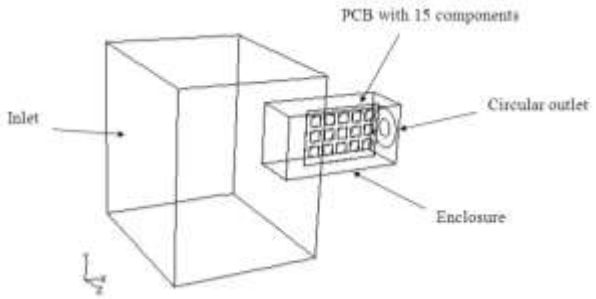

Figure 7. Model used to validate with previous experimental work.

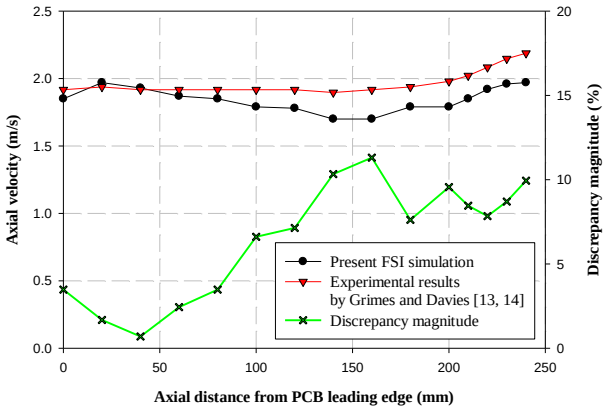

Figure 8. Axial velocity validation with previous experimental work along the Reference line.

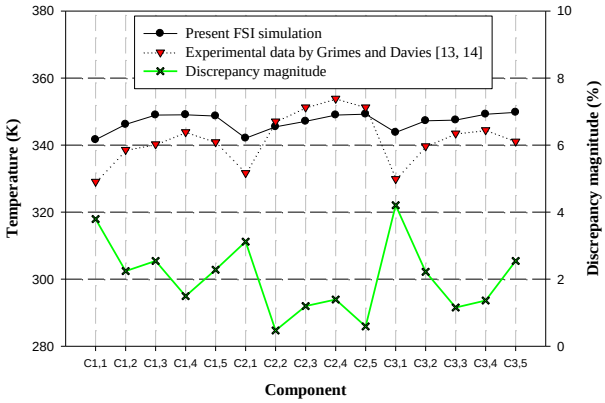

Figure 9. Temperature validation with previous experimental work.

RESULTS AND DISCUSSIONS

Deflection and Stress Distributions

For all the cases considered, the deflection and stress contour trends are almost identical because the fixed regions are unchanged. Figure 10 shows the deflection and stress distributions at final constant-state for Case A at 0.20 kg/s. It is noticed that most of the stresses are accumulated at the four corners of the constraint area. Higher deflections are found at the centre of the FPCB because it is located furthest away from the fixed constraints. In addition, Figures 11 and 12 describe the induced deflection and stress at different location in order to characterize the behavior of the FPCB. The column 4 components deflect slightly higher than the column 2 components, thereby resulting in higher stress at the trailing edge.

The deflection at different location of FPCB behaves identically, and the only prominent difference between them is their magnitudes. Same condition is also observed for the stress. Therefore, it is rational to use deflection at C2,3 and stress at Fix 2 to characterize the behavior of FPCB in the study, since they symbolize the critical location in the FPCB respectively. In practice, larger deflection is not favored because the FPCB can strike at the enclosure and then affecting the performance of the system. Larger stress is also undesirable in terms of reliability, and highly fluctuating stress is even worse due to fatigue consideration.

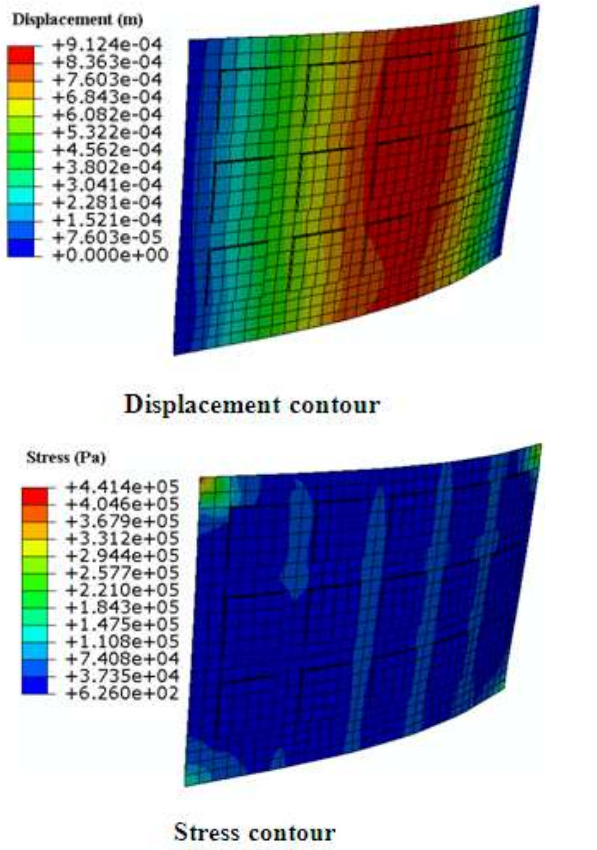

Figure 10. Deflection and stress contours at constant-state for Case A at 0.20 kg/s.

Effect of Mass Flow Rates

Effect of mass flow rates is carried out for Case A arrangement, and the results are shown in Figures 13 through 15. It is seen that, at higher flow rate, the induced deflection and stress become more vigorous, but the fluctuation time are significantly reduced. At flow rate of 0.25 kg/s, the maximum induced deflection and stress can attain until 1.4 mm and 0.85 MPa, respectively. The induced stress is not so alarming when comparing with yield strengths of polyimide (52-90 MPa)

(Ashby and Jones, 2005). However, the deflection issue must be given utmost care, especially in miniaturized

devices. Besides, it is also noted that upstream components are cooled more effectively compared to downstream components because downstream components are always exposed to heated air, which then decrease their heat transfer capabilities. So, the designer has to bear this idea in mind and give priority to locate the temperature sensitive component at the upstream.

Unfortunately, both maximum deflection (also maximum stress) and average heat transfer coefficient are increased with the flow rate, as depicted in Figure 16. The reason is that the higher flow rate provides more fresh air for removing the heat from the components, and the meanwhile also results in more flow impact. This situation implies that as flow rate decreases, the physical reliability can be improved but sacrifice has to be made on the cooling capability. At this juncture, the designer has to be aware about this issue (which is not a concern issue in conventional rigid PCB) and make compromise between these two parameters when dealing with FPCB electronics.

Effect of Inlet/Outlet Arrangements

Deflections and stresses

From Figures 17 and 18, it is clear that the different inlet/outlet arrangements have prominent effect on the induced deflection and stress. The results show Case C demonstrates the highest deflection and stress because the air directly impinges on the FPCB surface. Case B also provides comparable deflection and stress with Case C, but the deflection is in the opposite direction. This is due to the air enters from one side of the enclosure and then exits on the other side. Therefore, the FPCB deflected direction is not always the same; rather, it mainly depends on the manner by which the inlet and outlet are configured. On the other hand, Cases D and E exhibit significantly reduced the deflections and stresses because the air is now introduced in the vertical order (*y*-direction) without impinging on the FPCB surface. However, these configurations initiate unfavorable fluctuations on the deflections and stresses.

For Case A, it is noticed that it offers the best physical reliability with small deflection, small stress and also negligible fluctuation behavior.

From the results, it is worth noting that the maximum deflection and stress can achieve up to 3.3 mm and 4.1 MPa, respectively. Thus, these reliability issues are crucial and should not be ignored in the design of FPCB electronics. Moreover, the fluctuations of deflection and stress are also highly undesirable because extreme fatigue may deteriorate the reliability in the long run.

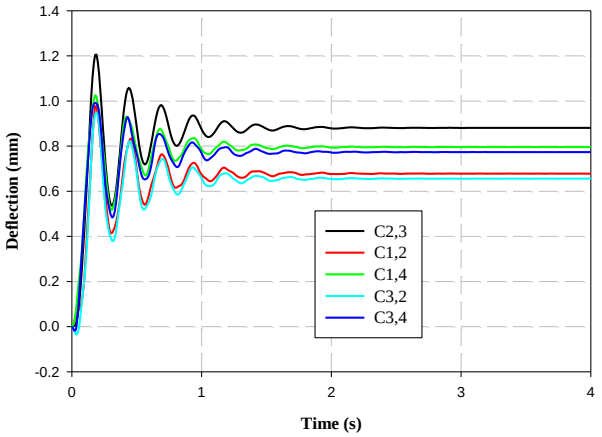

Figure 11. Deflections of different components for Case A at 0.20 kg/s.

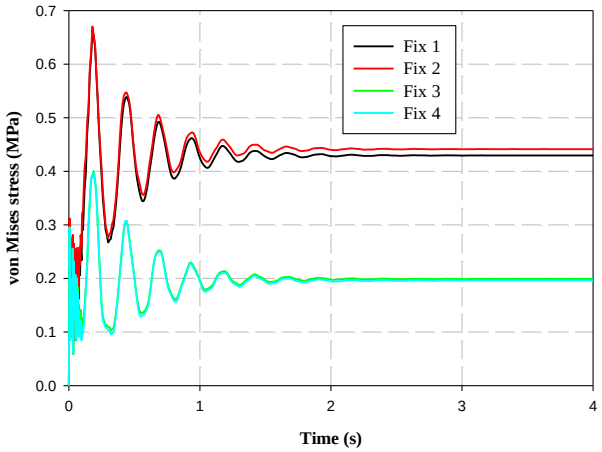

Figure 12. Stresses of different constraint locations for Case A at 0.20 kg/s.

Component temperatures

Figure 19 depicts the component temperatures for different inlet/outlet arrangements. The flows for different inlet/outlet arrangements are shown in Figure 20. The temperature distribution for Case A has been discussed in 'Effect of Mass Flow Rates' section.

For Cases D and E, the temperatures of row 1 components are remarkably higher. This is because, from inlets to outlets, the flow paths bypass the row 1 components, as clearly seen in the Figure 20. Besides

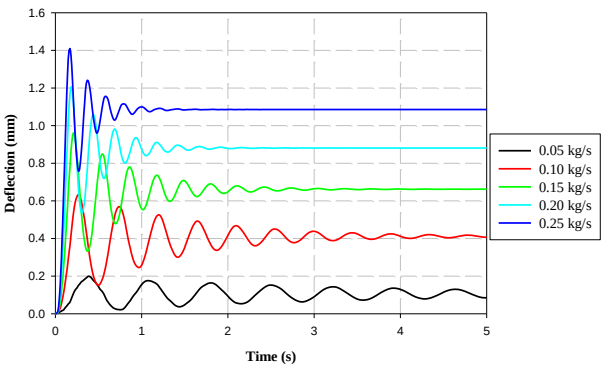

Figure 13. Deflections at different mass flow rates for Case A.

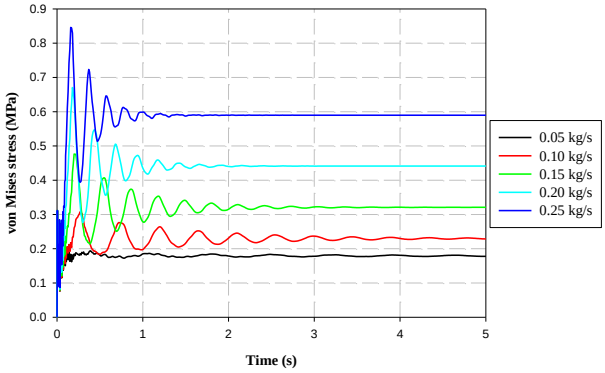

Figure 14. Stresses at different mass flow rates for Case A

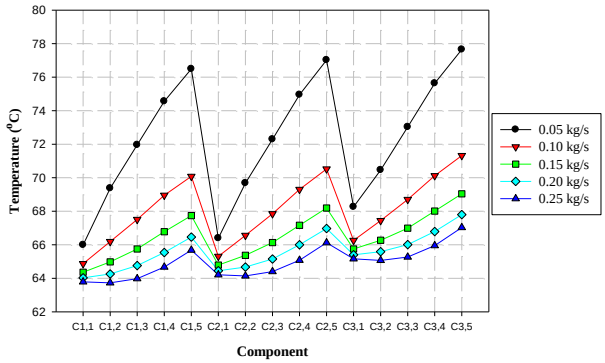

Figure 15. Component temperatures for different mass flow rates for Case A.

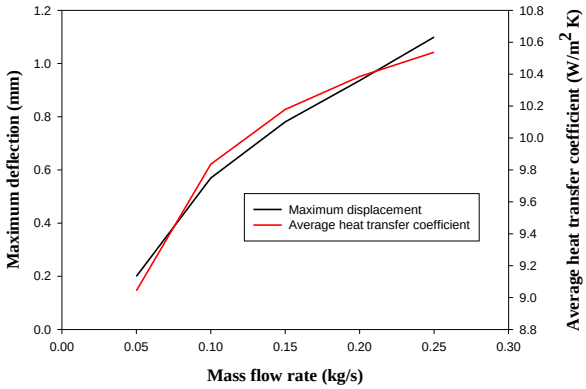

Figure 16. Change of maximum deflection and average heat transfer coefficient with mass flow rate for Case A.

that, the temperatures of the middle columns (2-4) components for most the cases are higher. The reason is that these components are located at the central of the FPCB, where they are barely protected from the main flows. However, Case C demonstrates opposite pattern, in which middle columns components exhibit lower temperatures, because of the perfect flow path as shown in Figure 21. Owing to this reason, the cooling performance for Case C is also enhanced. On the other hand, the flow in Case B is retarded when it tends to exit towards the other side of outlet. Also, the negatively deflected FPCB in Case B creates difficulty in cooling the components because the exposure of the components to the main flow is restricted. As a result, the cooling performance for Case B is greatly deteriorated. The average heat transfer coefficients for each case are also calculated and plotted in Figure 22.

Among the cases, it is discovered that Case C offers the best cooling performance and Case A rank the second.

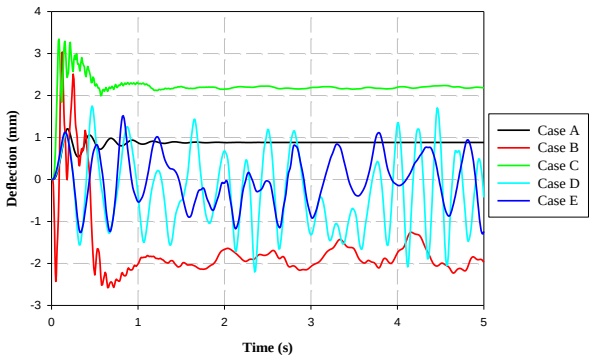

Figure 17. Deflections for different inlet/outlet arrangements.

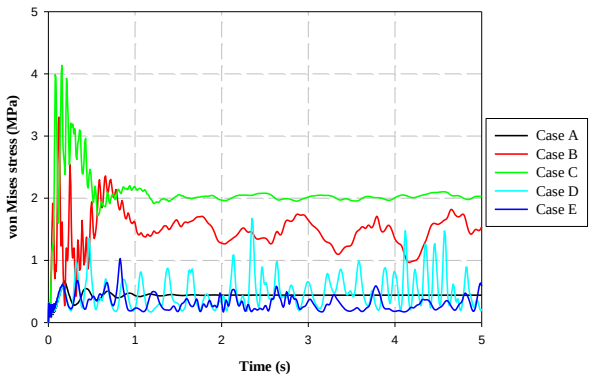

Figure 18. Stresses for different inlet/outlet arrangements.

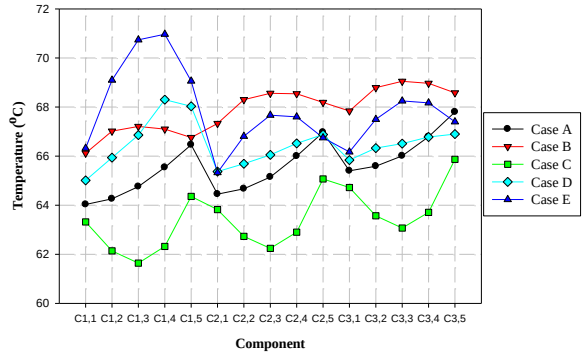

Figure 19. Component temperatures for different inlet/outlet arrangements.

Selection on different inlet/outlet arrangements

Cases D and E give undesirable high fluctuations of deflection and stress, which can lower the reliability of the FPCB. Moreover, these cases do not show any attractive in terms of cooling performance. Therefore, Cases D and E are not advisable to be used for FPCB electronic devices. It is also noticed that Cases B and C induce the highest deflection and stress. However, Case C offers the advantage of being the most effective in cooling among all cases. For Case A, it provides the best reliability and also promising cooling performance.

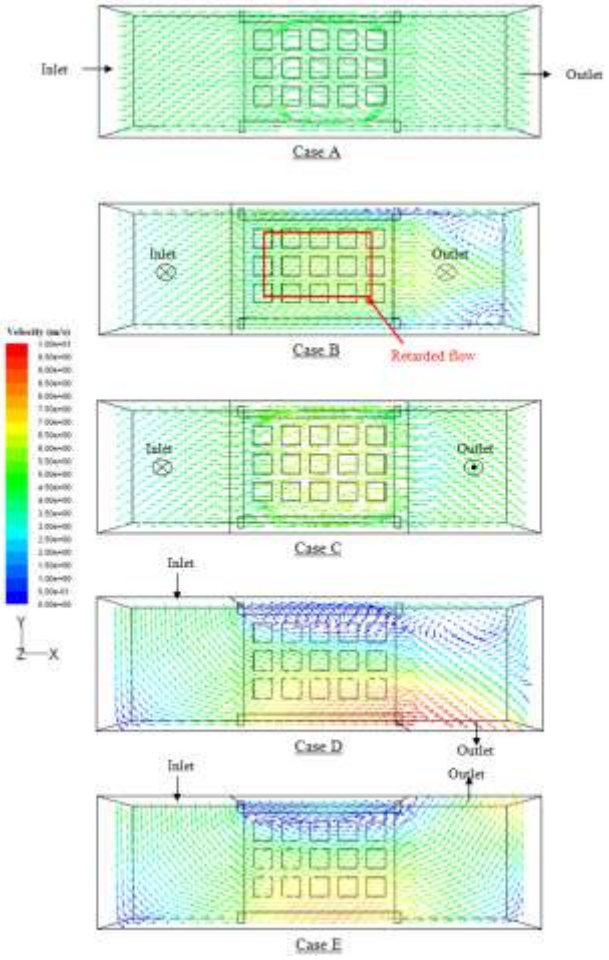

Figure 20. Flows in the enclosures for different inlet/outlet arrangements.

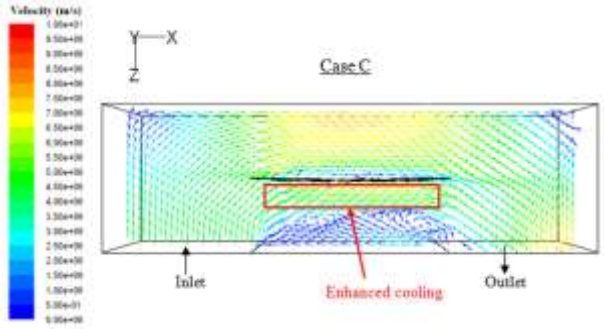

Figure 21. Top view of flow for Case C.

Consequently, Case A is the best selection by compromising the physical reliability and cooling performance. To maximize the cooling capability, Case C is reasonable to be considered, but it has to sacrifice with some reliability. However, if extra physical design or consideration is included to improve the FPCB stability, Case C can be given the first priority since it can offer excellent cooling capability. Therefore, apart from the Case A (axial flow), opportunity in enhancing the reliability and cooling performance can be achieved using Case C (U-flow perpendicular to FPCB) with additional stability.

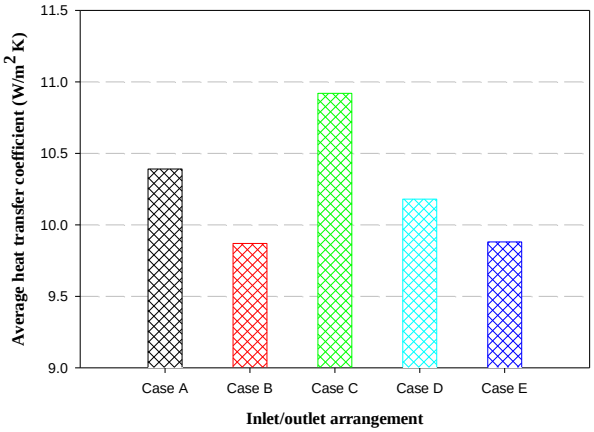

Figure 22. Average heat transfer coefficients for different inlet/outlet arrangements.

CONCLUSIONS

The fluid-structure interaction (FSI) numerical study is carried out on FPCB using FLUENT and ABAQUS; they are real-time online coupled by MpCCI. The present FSI simulation is validated against similar previous experimental work and shown in good agreement. The effect of mass flow rates and effect of air inlet/outlet arrangements are found to be influential on the reliability and cooling performance of FPCB. As air flow rate increases, it would help to increase the cooling capability, but the reliability would be deteriorated. Therefore, compromise between these two parameters is crucial when dealing with the FPCB electronics. In comparison of different air inlet/outlet arrangements, Case A arrangement (axial flow) demonstrates excellent performance in the application of FPCB electronics. However, the present study also explores the feasibility to enhance the reliability and cooling performance using extra stabilized Case C arrangement (U-flow perpendicular to FPCB). This study may be extended to investigate the FPCB in real life application product. Detailed experimental analysis may also be performed to substantiate the present predictions.

ACKNOWLEDGEMENT

The authors would like to thank Universiti Sains Malaysia, Penang, Malaysia, for the financial support for this research work, under the USM Fellowship scheme.

REFERENCES

Arruda L., Bonadiman R., Costa F. and Reinikainen T., 2009a, Cracking phenomena on flexible-rigid interfaces in PCBs under thermo cycling load, *Circuit World*, 35, 2, 28-22.

Arruda L., Chen Q. and Quintero J., 2009b, Failure evaluation of flexible-rigid PCBs by thermo-mechanical simulation, *International Conference on Electronic Packaging Technology & High Density Packaging*, 1201-1205.

Ashby M. F. and Jones D. R. H., 2005, *Engineering materials 1: An introduction to properties, applications and design* (Third edition), Oxford, UK.

Azar K and Russell E. T., 1990, Effect of component layout and geometry on the flow distribution in electronics circuit packs, *Sixth IEEE SEMI-THERM™ Symposium*, 1-9.

Baelmans M., Meyers J. and Nevelsteen K., 2003, Flow modeling in air-cooled electronic enclosures, *19th IEEE SEMI-THERM Symposium*, 27-34.

Barlow F., Lostetter A. and Elshabini A., 2002, Low cost flex substrates for miniaturized electronic assemblies, *Microelectronics Reliability*, 42, 1091-1099.

Bielecki M., Karcz M., Radulski W. and Badur J., 2001, Thermo-mechanical coupling between the flow of steam and deformation of the valve during start-up of the 200MW turbine, *Task Quarterly*, 5, 2, 125–140.

Cole R., Davies M. and Punch J., 2003, A board level study of an array of ball grid components- Aerodynamic and thermal measurements, *Journal of Electronic Packaging*, 125, 480-489.

Das R. N., Egitto F. D., Wilson B., Poliks M. D. and Markovich V. R., 2010, Development of rigid-flex and multilayer flex for electronic packaging, *Electronic Components and Technology Conference*, 568-574.

Eveloy V., Lohan J. and Rodgers P., 2000, A benchmark study of computational fluid dynamics predictive accuracy for component-printed circuit board heat transfer, *IEEE Transactions on Components and Packaging Technologies*, 23, 3, 568-577.

Fluent, 2012a, Modeling basic fluid flow. FLUENT Documentation [Chapter 9].

Fluent, 2012b, Modeling heat transfer. FLUENT Documentation [Chapter 13].

Grimes R., Davies M., Punch J., Dalton T. and Cole R., 2001, Modeling electronic cooling axial fan flows, *Journal of Electronic Packaging*, 123, 112-119.

Grimes R. and Davies M., 2002, The effect of fan operating point and location on temperature distribution in electronic systems, *Inter Society Conference on Thermal Phenomena*, 677-684.

Grimes R. and Davies M., 2004a, Air flow and heat transfer in fan cooled electronic systems, *Journal of Electronic Packaging*, 126, 124-134.

Grimes R. and Davies M., 2004b, Optical measurement of electronic system air flow and temperature distribution, *Journal of Optics A: Pure and Applied Optics*, 6, 617-626.

Han S., Seo K., Kim W., Lee H., Lee H., Shin J. and Lee J., 2007, Fatigue behavior of thin Cu foils for flexible printed circuit board, *Solid state Phenomena*, 124-126, 1369-1372.

Huang J., Chen Q., Xu L. and Zhang G.Q., 2009, Prediction of drop impact reliability of BGA solder joints on FPC, *11th Electronics Packaging Technology Conference*, 663-667.

Lau D., Chan Y. S., Ricky Lee S. W., Fu L., Ye Y. and Liu S., 2006, Experimental testing and failure prediction of PBGA package assemblies under 3-point bending condition through computational stress analysis, *7th International Conference on Electronics Packaging Technology*, 1-7.

Lee T. and Mahalingam M., 1993, Application of a CFD tool for system level thermal simulation, *IEEE*, 249-255.

Leicht L. and Skipor A., 2000, Mechanical cycling fatigue of PBGA package interconnects, *Miroelectronics Reliability*, 40, 1129-1133.

Leung C. W., Chen S. and Chan T. L., 2000, Numerical simulation of laminar forced convection in an air-cooled horizontal printed circuit board assembly, *Numerical Heat Transfer, Part A*, 37, 373-393.

Li R. S. and Jiao J., 2000, The effects of temperature and aging on Young's moduli of polymeric based flexible substrate, *The International Journal of Microcircuits and Electronic Packaging*,23, 4, 456-461.

Lohan J., Eveloy V. and Rodgers P., 2002, Visualization of forced air flows over a populated printed circuit board and their impact in convective heat transfer, *Inter Society Conference on Thermal Phenomena*, 501-511.

Odegard G. M., Clancy T. C. and Gates T. S., 2005, Modeling of the mechanical properties of nanoparticle/polymer composites, *Polymer*, 46, 553-562.

Rodgers P. J., V.C. Eveloy V. C. and Davies M. R. D., 2003a, An experimental assessment of numerical predictive accuracy for electronic component heat transfer in forced convection- Part I: Experimental methods and numerical modeling, *Journal of Electronic Packaging*, 125, 67-75.

Rodgers P. J., V.C. Eveloy V. C. and Davies M. R. D., 2003b, An experimental assessment of numerical predictive accuracy for electronic component heat transfer in forced convection- Part II: Results and discussion, *Journal of Electronic Packaging*, 125, 76-83.

Shankaran G. V. and Karimanal K., 2002, A multi level modeling approach with boundary condition import for system, sub-system or board level thermal characterization, *18th IEEE SEMI-THERM Symposium*, 35-41.

Shetty S., Lehtinen V., Dasgupta A., Halkola V. and Reinikainen T., Fatigue of chip scale package interconnects due to cyclic bending, *Journal of Electronic Packaging*, 123, 302-308.

Shetty S. and Reinikainen T., 2003, Three- and four-point bend testing for electronic packages, *Journal of Electronic Packaging*, 125, 556-561.

Siegel A. C., Phillips S. T., Dickey M. D., Lu N., Suo Z. and Whitesides G. M., 2010, Foldable printed circuit boards on paper substrates, *Advanced Functional Materials*, 20, 28-35.

Sun H.-b, Shi M.-q, Yang P., Zhong J., Chen Q., Xue T., Zhao T., Xu L. and Salo A., 2009, Rigid-flexible printed circuit structure optimization by simulations, *10th International Conference on Thermal, Mechanical and Multiphysics Simulation Experiment in Micro-Electronics and Micro-Systems*, 1-4.

Yeh C.-L., Lai Y.-S. and Kao C.-L., 2006, Evaluation of board-level reliability of electronic packages under consecutive drops, *Microelectronics Reliability*, 46, 1172-1182.

Yu D., Kwak J. B., Park S. and Lee J., 2010, Dynamic responses of PCB under product-level free drop impact, *Microelectronics Reliability*, 50, 1028–1038.